KSME International Journal, Vol. 13, No. 5, pp. 397~402, 1999

A Study on Tensile and Fatigue Properties of Aged NAS 254N Stainless Steel at Elevated Temperatures

Jae-Kyoo Lim*, Do-Won Seo and Zhong-Sen Li****

(Received June 13, 1998)

The effects of aging on tensile properties and fatigue crack growth behaviors of NAS 254N stainless steel was studied. Yield strength and ultimate tensile strength of the aged specimens were almost the same as the as-received(as-rec.). The fracture strain, however, was decreased significantly by the aging, and the fracture surface of the aged at room temperature(RT) test was intergranular. As test temperature increased, yield strength, ultimate tensile strength and elongation decreased. And a type of serration was observed at 550~650℃. As strain rate decreased, yield strength and ultimate tensile strength decreased, but elongation increased. It was observed that tensile strength and strain had a sudden change at one point. And this critical temperature T_{cr} was 550℃. The effect of aging time on the tensile strength and strain was also investigated. Tensile strength and strain decreased significantly beyond 100hrs. Fatigue crack growth rate at RT was enhanced by the aging at high stress intensity factor range. This is due to the occurrence of the intergranular fracture in the aged specimen. At 650℃, the fatigue crack growth behavior was almost the same without intergranular fracture.

Key Words: NAS 254N Stainless Steel, Aging, Strain Rate, Elevated Temperatures, Tensile Properties, Fatigue Crack Growth, Intergranular Fracture

1. Introduction

NAS 254N stainless steel has been used over a very wide temperature range, being utilized at room and elevated temperatures in machines, chemical and power plants. These components are experiencing the stressing at various temperatures and different strain rates in service. Furthermore, the components are subjected to cyclic loading and aggressive environments during service which could result in crack-like defects. To evaluate the structural integrity, not only tensile mechanical properties but also the fatigue crack growth behaviors after long time service should be known.

Degradation of the stainless steel properties due to long service exposure (Sikka, 1978) and due to simulated aging (Balladon, 1986) has been reported. Sikka observed the decrease in tensile ductility of 316 stainless steel by 51,000hrs exposure. Balladon reported that elastic-plastic fracture toughness J_{IC} at room and elevated temperatures are decreased by aging from 1,000 to 10,000hrs. The service-exposed material suffers not only high temperature aging but also thermal and mechanical stress. It would be of importance, therefore, to assess the mechanical properties of the serviced materials.

In this study, therefore, tensile and fatigue test at elevated temperatures and scanning electron microscope(SEM) analysis were performed to find out the effects of temperature, heat treatment and strain rate on the mechanical properties of super austenitic stainless steel.

* Automobile Hi-Technology Research Institute and Dept. of Mechanical Design, Chonbuk Nat'l Univ., Chonju, 561-756, Korea

** Graduate school, Dept. of Mechanical Eng., Chonbuk Nat'l Univ., Chonju, 561-756, Korea

2. Experimental Method

2.1 Specimens

The material used was a commercially available NAS 254N stainless steel(t=18mm). It has more Ni, Cr and N than other components of austenitic stainless steel to be in use at high Cl- environment. Chemical compositions(wt.%) of the steel are shown in Table 1. Isothermal aging heat treatment was carried out at 650℃ in air for 100hrs, 240hrs and 1,000hrs.

The smooth cylindrical tensile specimen(5.6mm diameter and 20mm gauge length) was machined from the plate such that the specimen axis was parallel to the rolling direction. 0.8T compact tension(CT) specimen with notch was machined by an electric discharge wire-cut machine. Pre-fatigue crack of CT specimen was introduced in accordance with the ASTM standard(ASTM E 399-90) using a servo controlled electro-hydraulic fatigue testing machine. The notch root was mechanically polished with emery papers.

2.2 Test conditions

Tensile test was carried out using a 5-ton screw-driven machine on the displacement control. For the as-received specimens, the test was performed at room temperature(RT, 20-23℃), 350, 550, 650 and 750℃ under strain rate=4.17×10^{-2}, 4.17×10^{-4} and $4.17\times 10^{-6}s^{-1}$, respectively. But for the aged specimens, it was done at RT and 650℃ only. Strain rate ε is defined as the ratio of the cross head speed(CHS) to the gauge length 20mm of the tensile specimen. An electric furnace was used for the elevated temperature test. The temperature was controlled within ±5℃. The loading started after 30min. of holding time at the test temperature and continued up to either maximum load or complete fracture. The presence of serrations was established from the load-displacement curves recorded on charts. After the test, diameter of gauge length part was measured using a stereoscope and a profile projector.

Tensile mechanical properties determined include yield stress σ_y, ultimate tensile strength UTS, ultimate true tensile strength σ_{ut} (σ_{ut}= maximum load/A_{UTS}, where A_{UTS} is the area at UTS), fractured true stress σ_f, elongation to failure e_f (the ratio of the actual elongation to the gauge length), uniform strain ε_u ($\varepsilon_u=\ln(1+e_{UTS})$, where e_{UTS} is the engineering strain at UTS), and fractured true strain ε_f.

A fatigue test was performed on the precracked CT specimen at RT and 650℃, using an electro-hydraulic servocontrolled MTS fatigue machine with electric furnace under load control of the range 3920~220.5N and 1960~122.5N, respectively. In order to find out the effect of aging time, the as-received and the aged(240 and 1,000hrs) specimens were tested. The waveform was sinusoidal, and the frequency was 1 to 5Hz. During the fatigue test the notch root was observed using a stereoscope, thus crack length vs cycles data were taken.

Table 1 Chemical compositions (wt. %)

C	Si	Ni	Cr	Mo	N	S
0.008	0.4	25	23	5.5	0.2	≤0.001

3. Results and Discussion

3.1 Load-displacement curves

Load-displacement curves of the as-received

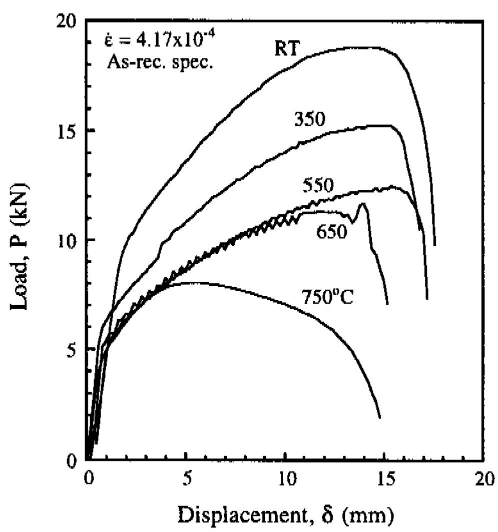

Fig. 1 Load-displacement curves at various temperature at $\varepsilon=4.17\times 10^{-4}s^{-1}$.

specimens at strain rate $\varepsilon=4.17\times10^{-4}s^{-1}$ with various temperatures are illustrated in Fig. 1. The temperature dependence of the properties at this strain rate is as follows: 1) a serrated flow is observed at two temperature ranges, the first weak flow at 350℃ and the second in the range 550 ~650℃, 2) above 650℃, *UTS* and work hardening decrease rapidly as test temperature increases. The tendency of the temperature dependence of the behaviour at other strain rates was the same as at $\varepsilon=4.17\times10^{-4}s^{-1}$.

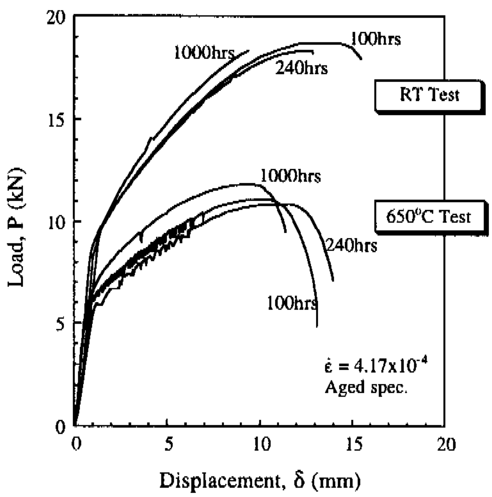

Fig. 2 Load-displacement curves for various aging time at RT and 650℃.

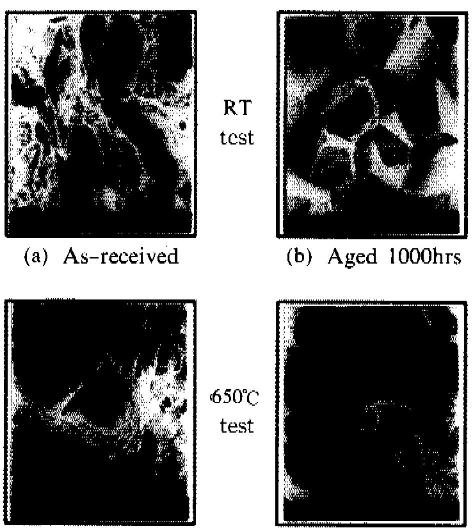

(a) As-received (b) Aged 1000hrs

(c) As-received (d) Aged 1000hrs

Fig. 3 Tensile fracture appearance at $\varepsilon=4.17\times10^{-4}s^{-1}$
(a) as-received, (b) aged(650℃)
(c) as-received, (d) aged(650℃)

Load-displacement curves of the aged specimens, at various aging time under strain rate $\varepsilon=4.17\times10^{-4}s^{-1}$ and two test temperature RT and 650℃, are illustrated in Fig. 2. In the case of testing at 650℃, the value of yield strength and *UTS* are decreased significantly compared with those of RT test, and serrated flow is observed at aging time 100hrs and 240hrs.

Fracture surface micrographs by SEM are illustrated in Fig. 3. The fracture surfaces of the aged (1,000hrs) specimen tested at RT represents intergranular fracture. At 650℃ test, however, the fracture surfaces of the as-received and aged(1,000hrs) specimen are ductile fracture with dimples.

3.2 Tensile strengths

The strain rate and temperature dependence of σ_f, σ_{ut}, *UTS* and σ_y for the as-received are shown in Fig. 4. All strengths at RT are the highest than other test temperatures. Strain rate effect is remarkable on σ_{ut} and *UTS*, and not so much on σ_y and σ_f. It should be noted, however, that at 550℃ both σ_{ut} and *UTS* are constant and independent of ε. At this temperature, ductilities are also independent of ε as shown later. The temperature is therefore denoted here after as the critical temperature T_{cr}. Below T_{cr}, all strengths

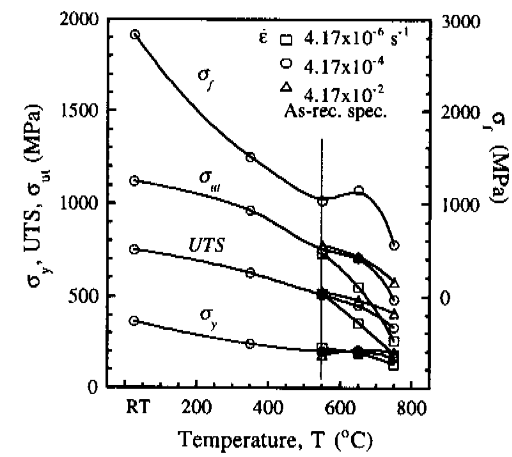

Fig. 4 Temperature T and strain rate ε dependences of yield stress σ_y, ultimate tensile strength *UTS*, ultimate true stress σ_{ut} and fractured true stress σ_f.

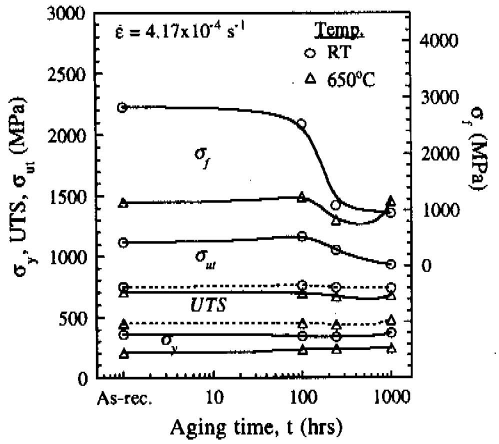

Fig. 5 Aging time t and temperature T dependences of yield stress σ_y, ultimate tensile strength UTS, ultimate true stress σ_{ut} and fractured true stress σ_f.

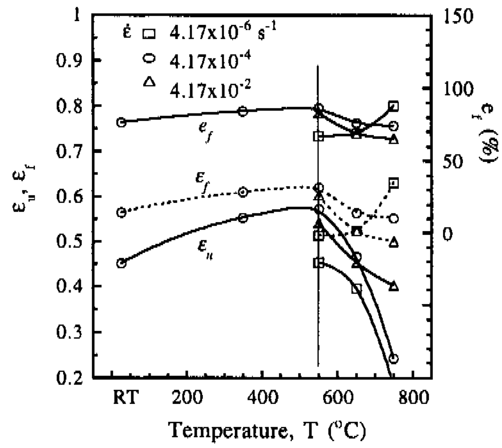

Fig. 6 Temperature T and strain rate ε dependences of uniform strain ε_u, fractured elongation e_f and fractured true strain ε_f.

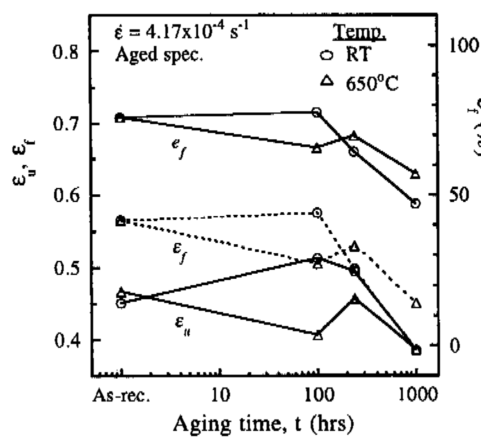

Fig. 7 Aging time t and temperature T dependences of uniform strain ε_u, fractured elongation e_f and fractured true strain ε_f.

increase almost linearly originating from the point T_{cr}. Above 650℃, they decrease rapidly with increasing temperature, and the lower the strain rate, the lower the strength.

The aging time and temperature dependence of σ_f, σ_{ut}, UTS and σ_y for the aged at $\varepsilon = 4.17 \times 10^{-4}\mathrm{s}^{-1}$ are shown in Fig. 5. Strengths at RT are higher than those at 650℃. From 0(the as-received) to 100hrs, all strengths are almost constant at both RT and 650℃, independent of aging time. At 100hrs, σ_f and σ_{ut} start decreasing rapidly with increasing aging time, but UTS and σ_y are constant.

3.3 Ductilities

For the as-received, the effects of temperature and strain rate on e_f, ε_f and ε_{ut} are shown in Fig. 6. It is seen that all ductilities have a peak point at T_{cr}(550℃) and are almost independent of ε, a same tendency has also been observed in strengths except for $\varepsilon = 4.17 \times 10^{-6}\mathrm{s}^{-1}$. Below T_{cr}, all strengths (at $\varepsilon = 4.17 \times 10^{-4}\mathrm{s}^{-1}$) increase almost linearly.

The effects of aging time and temperature on e_f, ε_f and ε_{ut} at $\varepsilon = 4.17 \times 10^{-4}\mathrm{s}^{-1}$ are shown in Fig. 7. For the as-received materials, both e_f and e_f are constant and independent of testing temperature. From as-received to 100hrs, e_f and e_f at RT test are almost constant, but above 100hrs, they decrease rapidly with increasing aging time. This is due to the occurrence of the intergranular fracture of the aged (240, 1,000hrs) specimen tested at RT, but the as-received and aged (100hrs) specimens are ductile fracture with dimples.

3.4 Fatigue crack growth behavior

Figure 8 shows the relation between the fatigue crack growth rate da/dN and the stress intensity factor range ΔK at RT. An approximately linear relationship is observed between log (da/dN) and log (ΔK). Below $\Delta K = 28\mathrm{MPa} \cdot \mathrm{m}^{1/2}$, the as-received and the aged (240 and 1,000hrs) specimens are almost the same. Above $30\mathrm{MPa} \cdot \mathrm{m}^{1/2}$,

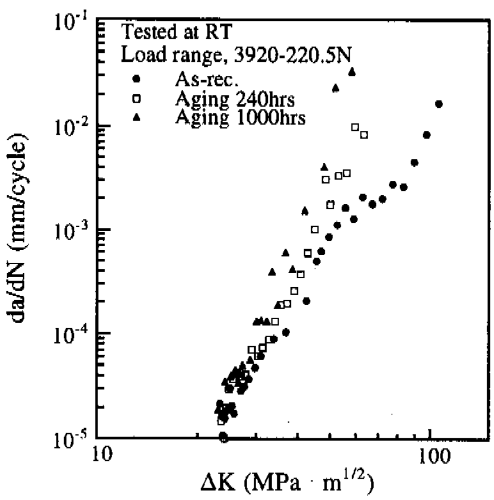

Fig. 8 Relation between stress intensity factor range ΔK and fatigue crack growth rate da/dN at RT.

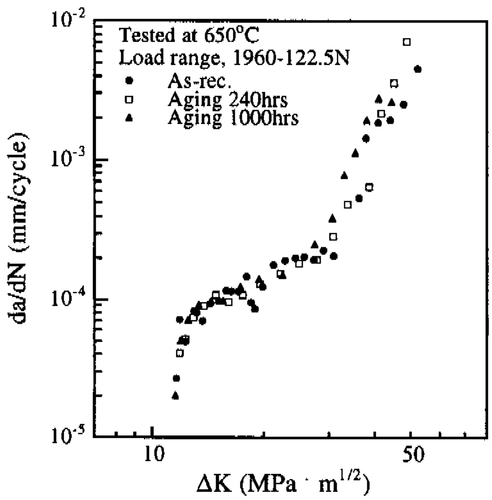

Fig. 9 Relation between stress intensity factor range ΔK and fatigue crack growth rate da/dN at 650℃.

however, the da/dN of the aged specimens is larger than that of the as-received; and the higher ΔK, the larger difference between both da/dN. At $\Delta K = 60\text{MPa} \cdot \text{m}^{1/2}$, the da/dN of the aged (1,000hrs) is over 10 times compared with the as-received. In the SEM fractographs analysis, the as-received materials exhibited striation in transgranular fracture made on the fracture surface. Below $da/dN = 10^{-4}$mm/cycle, the fracture surface of the aged at RT test was transgranular; above that ($\Delta K > 30\text{MPa} \cdot \text{m}^{1/2}$), however, the fracture was mostly intergranular; i.e., fatigue crack growth rate at RT is enhanced by aging at high stress intensity factor range. This is due to the occurrence of the intergranular fracture in the aged specimen.

As shown in Fig. 9, at 650℃, the fatigue crack growth behavior of the as-received and the aged (240 and 1,000hrs) specimens was almost the same tendency over all of the stress intensity factor range without intergranular fracture.

4. Conclusions

The effects of aging on tensile properties and fatigue crack growth behaviors of NAS 254N stainless steel was studied. The results are summarized as follows.

(1) For tensile test of the as-received specimens at RT and $\dot{\varepsilon} = 4.17 \times 10^{-4}\text{s}^{-1}$, serrated tendency was observed at temperature 350℃ and 550-650℃. And for the aged at 650℃, it was represented at aging time 100 and 240hrs.

(2) At 550℃, both σ_{ut} and UTS of the as-received are constant and independent of $\dot{\varepsilon}$. At this temperature, ductilities are also constant and independent of $\dot{\varepsilon}$. The temperature is therefore denoted the critical temperature T_{cr}.

(3) σ_f, σ_{ut}, UTS and σ_y for the aged specimens at $\dot{\varepsilon} = 4.17 \times 10^{-4}\ \text{s}^{-1}$, from aging time 0 (as-rec.) to 100hrs, are almost constant at both RT and 650℃. They are independent of aging time.

(4) Fatigue crack growth rate at RT was enhanced by aging at high stress intensity factor range. This is due to the occurrence of the intergranular fracture in the aged specimen. At 650℃, fatigue crack growth behavior was almost the same without intergranular fracture.

References

ASTM Standards, 1993, "Test Method for Plane-Strain Fracture Toughness of Metallic Materials," *ASTM E 399-90*.

Balladon, P. and Heritier, J., 1986, "Comparison of Ductile Crack Growth Resistance of Austenitic, Niobium-stabilized Austenitic and Austeno-ferritic Stainless Steels," *Fracture Mechanics, ASTM STP 905*, pp. 661～682.

Iino, Y., 1986, "Tensile Properties of Type 304 Stainless Steel in Temperature Range 77 to 1223K and Strain Rate Range 10^{-6} to 10^{-1} s^{-1}," *Bulletin of JSME*, Vol. 29, No. 248, pp. 355～361.

Iino, Y. and Suzuki K., 1988, "Notched Tensile Strength and Plastically Deformed Zone of Type 304 Stainless Steel at 4K," *Proceedings of the* VI *International Congress on Experimental Mechanics*, Vol. 1, SEM Inc., pp. 106～111.

Iino, Y., 1992, "Effect of Small and Large Amounts of Prestrain at 295K on Tensile Properties at 77K of 304 Stainless Steel," *JSME International Journal*, Series I, Vol. 35, No. 3, pp. 303～309.

James, L. A. and Schwenk, E. B., 1971, "Fatigue-Crack Propagation Behavior of Type 304 Stainless Steel at Elevated Temperatures," *Metallurgical Transactions*, Vol. 2, pp. 491～496.

Lim, J. K., Chang, J. S. and Iino, Y., 1997, "Evaluation of Elastic-Plastic Fracture Toughness of Aged AISI 316 Steel using DC-Electric Potential Method," *Transactions of the KSME*, Vol. 21, No. 3, pp. 519～527.

Lim, J. K., Hwang, S. J. and Lee, O. Y., 1997, "A Study on Fatigue Fracture Behaviour of 7000 Series Aluminum Alloys using Numerical Procedure," *Transactions of the KSME*, Vol. 21, No. 4, pp. 688～696.

Nakajima, Y., Iino, Y. and Suzuki, M., 1989, "Fracture Toughness Behaviour of Service-Exposed Type 321 Stainless Steel at Room and Elevated Temperature under Normal and Low Straining Rates," *Engineering Fracture Mechanics*, Vol. 33, No. 2, pp. 295～307.

Sikka, V. K., 1978, "Elevated Temperature Ductility of types 304 and 316 Stainless Steel, in *Ductility and Toughness Consideration in Elevated Temperature Service,*" *ASME*, pp. 129～148.